

A High-Affinity Human Antibody That Targets Tumoral Blood Vessels

By Lorenzo Tarli, Enrica Balza, Francesca Viti, Laura Borsi, Patrizia Castellani, Dietmar Berndorff, Ludger Dinkelborg, Dario Neri, and Luciano Zardi

Angiogenesis is a characteristic feature of many aggressive tumors and of other relevant disorders. Molecules capable of specifically binding to new-forming blood vessels, but not to mature vessels, could be used as selective vehicles and would, therefore, open diagnostic and therapeutic opportunities. We have studied the distribution of the ED-B oncofetal domain of fibronectin, a marker of angiogenesis, in four different tumor animal models: the F9 murine teratocarcinoma, SKMEL-28 human melanoma, N592 human small cell lung carcinoma, and C51 human colon carcinoma. In all of these experimental models we observed accumulation of the fibronectin isoform containing the ED-B domain around neovascular structures when the tumors were in the exponentially growing phase, but not in the slow-growing phase. Then we performed biodistribution studies in mice bearing a subcutaneously implanted F9 murine teratocarcinoma, using a high-affinity human antibody fragment (L19) directed against the ED-B domain of fibronectin. Radiolabeled L19,

TUMORS CANNOT GROW BEYOND a certain mass without the formation of new blood vessels (angiogenesis), and a correlation between microvessel density and tumor invasiveness has been reported for a number of tumors.¹ Molecules capable of selectively targeting markers of angiogenesis would create clinical opportunities for the diagnosis and therapy of tumors and other diseases characterized by vascular proliferation, such as rheumatoid arthritis, diabetic retinopathy, and age-related macular degeneration.²⁻⁸

The ED-B domain of fibronectin, a sequence of 91 amino acids identical in mice, rats, and humans, which is inserted by alternative splicing into the fibronectin molecule, specifically accumulates around neovascular structures⁹⁻¹² and could represent a target for molecular intervention. Indeed, we have recently shown with fluorescent techniques that anti-ED-B single-chain Fv antibody fragments (scFv¹³) injected in tumor-bearing mice selectively accumulate around tumoral blood

but not an irrelevant anti-lysozyme antibody fragment (D1.3), efficiently localizes in the tumoral vessels. The maximal dose of L19 accumulated in the tumor was observed 3 hours after injection (8.2% injected dose per gram). By virtue of the rapid clearance of the antibody fragment from the circulation, tumor-to-blood ratios of 1.9, 3.7, and 11.8 were obtained at 3, 5, and 24 hours, respectively. The tumor-targeting performance of L19 was not dose-dependent in the 0.7 to 10 μ g range of injected antibody. The integral of the radioactivity localized in tumoral vessels over 24 hours was greater than 70-fold higher than the integral of the radioactivity in blood over the same time period, normalized per gram of tissue or fluid. These findings quantitatively show that new-forming blood vessels can selectively be targeted *in vivo* using specific antibodies, and suggest that L19 may be of clinical utility for the immunoscintigraphic detection of angiogenesis in patients.

© 1999 by The American Society of Hematology.

vessels. Antibody affinity appears to dictate targeting performance.¹⁴ However, a quantitative measure of the dose of angiogenesis-specific antibody that can be delivered to the tumor is still missing. This issue is of fundamental interest, considering that blood vessels represent only a small percent of the total tumor mass and that *in vivo* detection of new-forming blood vessels crucially depends on the efficiency by which they can be targeted.

In this report, we have studied the distribution of the ED-B containing fibronectin (B-FN) in four different tumor animal models and we have quantitatively investigated the tumor-targeting properties of a radiolabeled anti-ED-B antibody fragment with affinity in the picomolar range.

MATERIALS AND METHODS

Animal models and antibodies. The four different tumor models were obtained by subcutaneous injection of the following cell lines in nude mice. The C51 human colon adenocarcinoma¹⁵ was kindly provided by Dr M. Colombo (Istituto Nazionale Tumori, Milano, Italy); the F9 mouse teratocarcinoma and the SKMEL-28 human melanoma were purchased from American Type Culture Collection (ATCC; Rockville, MD); the N592 human small cell lung carcinoma (SCLC) was kindly provided by Dr J.D. Minna (National Cancer Institute [NCI], Bethesda, MD).¹⁶ The monoclonal rat antibody MEC 13.3 to mouse CD31 (endothelial cell marker) was a kind gift of Drs A. Mantovani and A. Vecchi (Istituto Mario Negri, Milano, Italy).¹⁷ The monoclonal antibody (MoAb) Ki67 specific for proliferating cells was purchased from Dako (Carpinteria, CA). The preparation and characterization of scFv L19 has previously been reported.¹⁸

Immunohistochemistry. Immunohistochemical studies were performed as described.^{9,11}

Biodistributions of tumor-bearing mice injected with radiolabeled antibody fragments. ScFv(L19)¹⁸ (EMBL accession no. AJ006113) and scFv(D1.3)¹⁹ were affinity purified on an antigen column¹⁴ and radiolabeled with iodine-125 using the Iodogen method²⁰ (Pierce, Rockford, IL). Radiolabeled antibody fragments retained greater than 80% immunoreactivity, as evaluated by loading the radiolabeled antibody onto an antigen column, followed by radioactive counting of the flow-through and eluate fractions.

From Institut für Molekularbiologie und Biophysik, ETH Hönggerberg, Zürich, Switzerland; Istituto Nazionale per la Ricerca sul Cancro, Genova, Italy; and Research Laboratories of Schering AG, Berlin, Germany.

Submitted August 7, 1998; accepted March 3, 1999.

L.T. and E.B. have contributed equally to this work.

Supported by the EU Biotech Project "Novel Markers of Angiogenesis" (L.Z., D.N.), the Stiftung zur Krebsbekämpfung (D.N.), Associazione Italiana per la Ricerca sul Cancro (L.Z.) and the ETH Zürich (D.N.).

Address reprint requests to Dario Neri, PhD, Institut für Molekularbiologie und Biophysik, ETH Hönggerberg, CH-8093 Zürich, Switzerland; e-mail: dario@mol.biol.ethz.ch.

The publication costs of this article were defrayed in part by page charge payment. This article must therefore be hereby marked "advertisement" in accordance with 18 U.S.C. section 1734 solely to indicate this fact.

© 1999 by The American Society of Hematology.

0006-4971/99/9401-0030\$3.00/0

Nude mice (12-week-old Swiss nudes, males) with subcutaneously implanted F9 murine teratocarcinoma^{11,14} were injected with 3 μg (3 to 4 μCi) of scFv in 100 μL saline solution. Tumor size was 50 to 250 mg, because larger tumors tend to have a necrotic center. However, targeting experiments performed with larger tumors (300 to 600 mg) gave essentially the same results (data not shown). Tumors were measured with a dial-caliper and the volume was determined using the formula: $\text{Width}^2 \times \text{Length} \times 0.52$. Three animals were used for each time point. Mice were killed at 0.25, 1, 3, 5, and 24 hours after injection, the organs were weighed, and the radioactivity was counted. Targeting results of representative organs are expressed as percent of the injected dose of antibody per gram of tissue (%ID/g).

Animal experiments were performed according to the license "Tumor Targeting," issued to Dario Neri by the Veterinäramt des Kantons Zürich (Bewilligung 53/97).

To evaluate whether the tumor-targeting properties of L19 were dose dependent, biodistribution studies were performed at 24 hours, injecting tumor-bearing mice (CD1 nude females; 3 to 4 mice for each dose) with radioiodinated L19 (specific activity: 1 μCi of ¹²⁵I

for each μg of scFv) in a dose ranging between 0.7 and 10 μg per mouse.

Kinetic dissociation constant measurements. The binding properties of scFv(L19) to recombinant ED-B were studied by real-time interaction analysis with surface plasmon resonance detection using a BIAcore 1000 instrument (Biacore AB, Uppsala, Sweden) as described.¹⁴

The kinetic dissociation constant k_{off} of the scFv(L19)/ED-B complex was measured by competition. A 100 nmol/L biotinylated ED-B¹⁴ solution was applied to a streptavidin-coated microtiter plate (cat. no. 1645 692; Boehringer, Mannheim, Germany). After blocking for 30 minutes with a 2% solution of bovine serum albumin in phosphate-buffered saline (B-PBS), radioiodinated scFv(L19) in B-PBS (0.3 μg , 0.33 μCi) was added to each well, incubated at room temperature for 30 minutes, then washed three times with PBS + 0.1% Tween-20 and three times with PBS. To each well, a 10- $\mu\text{mol/L}$ solution of recombinant ED-B in B-PBS was then added at different times, in triplicate. At the end of the competition, wells were washed, cut, and then radioactivity counted in a gamma counter.

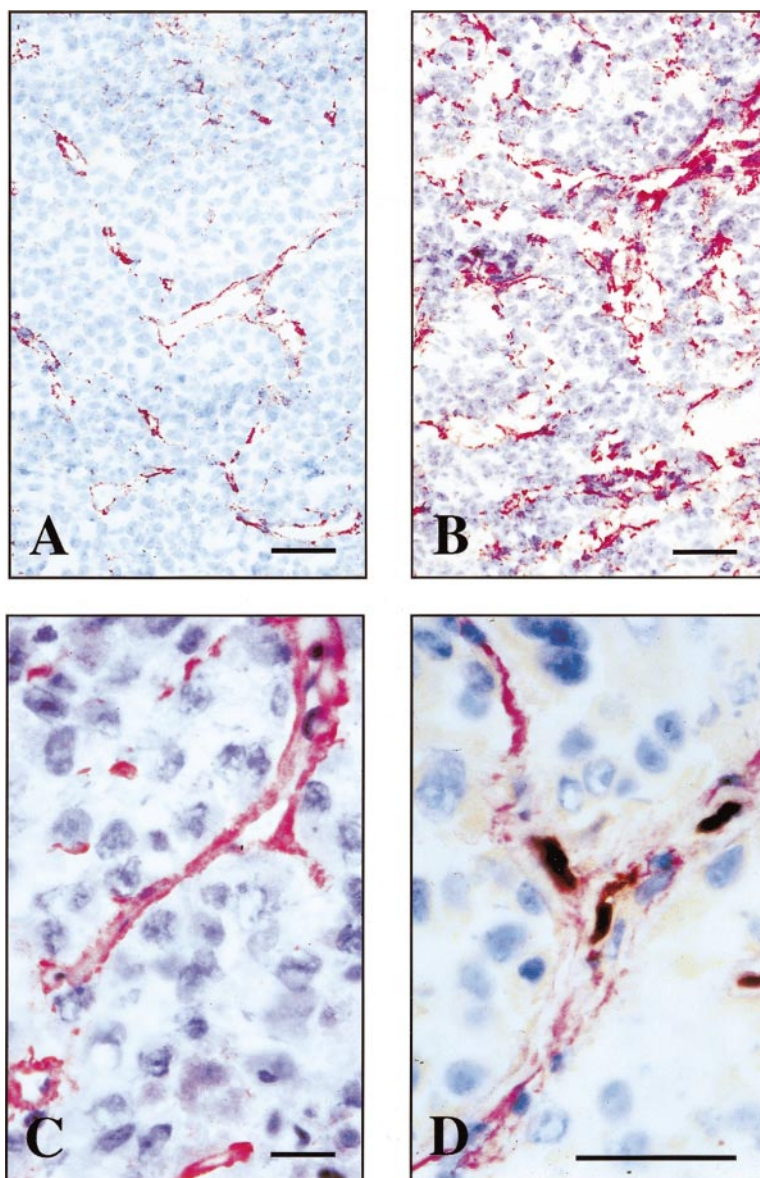


Fig 1. Immunohistochemical analysis of the distribution of B-FN in human and mouse grafted tumor models. Immunostaining of cryostat sections of F9 mouse teratocarcinoma allograft (A), N592 human small cell lung carcinoma xenograft (B), and SKMEL-28 human melanoma (C) using the antibody fragment L19. (D) A double staining of the SKMEL-28 human melanoma xenograft using the antibody fragment L19 (red staining) and an MoAb to mouse CD31, a marker of endothelial cells (brown staining). Scale bars: A, B, and D: 10 μm ; C: 4 μm .

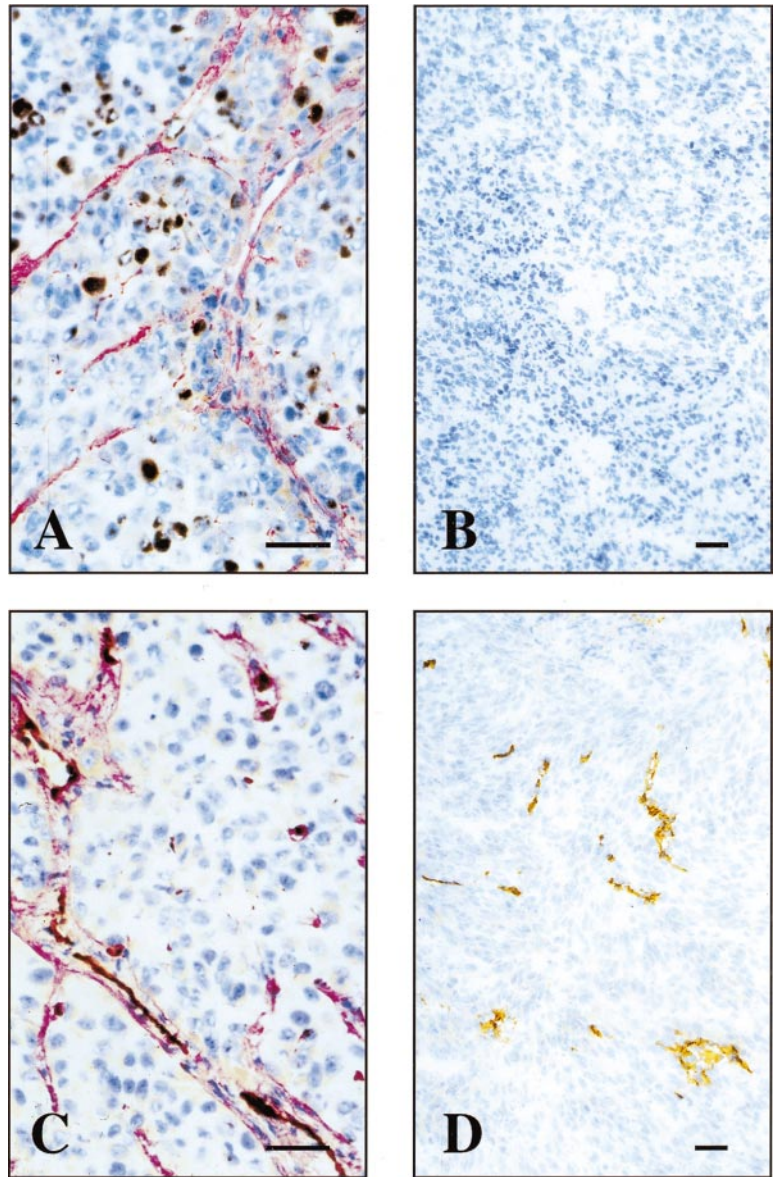


Fig 2. B-FN accumulates around the vessels of exponentially growing tumors but not on vessels of quiescent tumors. Cryostat sections of the SKMEL-28 xenograft in the exponentially growing phase (A and C) and in the quiescent phase (B and D). Sections shown in (A) and (B) were double stained using the antibody fragment L19 to B-FN (red staining) and the MoAb Ki67 specific for proliferating cells (brown staining). Sections shown in (C) and (D) were double stained using the antibody fragment L19 to BFN (red staining) and a rat MoAb recognizing murine CD31, a marker of endothelial cells (brown staining). The bar corresponds to 10 μ m.

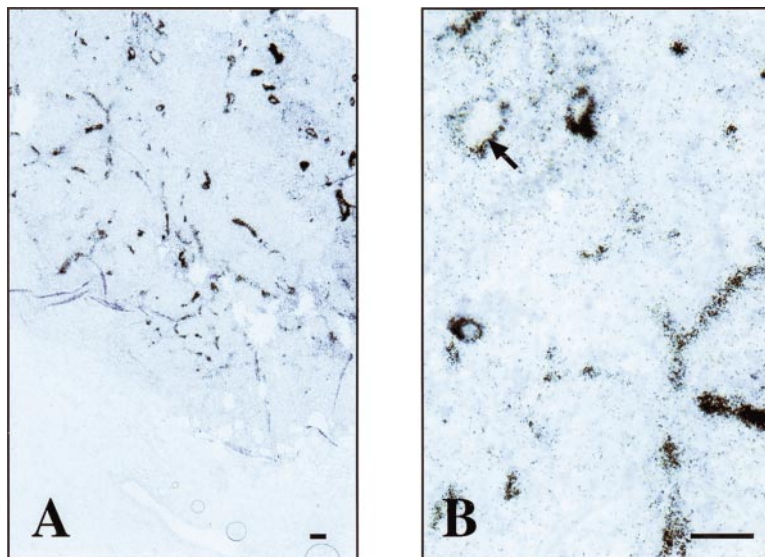


Fig 6. Microautoradiography of an F9 teratocarcinoma dissected from a nude mouse, after injection of radiolabeled L19. Two different magnifications of a microautoradiography of a F9 mouse teratocarcinoma. The radiolabeled L19 accumulates around vascular structures within the F9 mouse tumor but not in the surrounding normal mouse tissue (A). At higher magnification (B) within the lumens of some vessels, the red blood cells are visible (arrow). The bar corresponds to 10 μ m.

Microautoradiography studies. Selected tumor specimens were processed for microautoradiography to assess the pattern of ^{125}I -L19 distribution within tumors as a result of specific binding to the antigen. After alcohol dehydration, tissue samples were embedded in paraffin and sequentially sectioned (semi-thin sections, 5- μm thick), coated with NTB-2 emulsion (Kodak, Rochester, NY; diluted with distilled water 1/1.5), dried, and stored at 4°C in light-tight boxes. After exposure of approximately 2 to 3 weeks in the dark, the emulsions were developed (Kodak developer D-19B) for about 5 minutes at 19°C and fixed (Kodak Unifix for Kodak F-5 fixer) for 10 minutes. Finally, the slides were rinsed, stained with hematoxylin and eosin, and mounted in glycerol (Dako).²¹

RESULTS

Animal models and immunohistochemical studies. Using protein engineering techniques and phage display libraries,²² we have recently isolated a human antibody fragment, scFv(L19), which binds to the ED-B domain of fibronectin with extremely high affinity ($K_d = 54 \text{ pmol/L}$).¹⁸ The L19 antibody fragment was used to study immunohistochemically the distribution of B-FN in four animal models: the F9 murine teratocarcinoma, SK-MEL28 human melanoma, N592 human small cell lung carcinoma, and C51 human colon carcinoma. In all of these tumors, we observed accumulation of the B-FN around neovascular structures. Figure 1 shows the immunostaining of cryostat sections obtained from a F9 mouse teratocarcinoma allograft (A), N592 human small cell lung carcinoma xenograft (B), and from an SKMEL-28 human melanoma xenograft (C). In all these tumors, L19 stained vascular structures; similar results were obtained using the C51 human colon carcinoma xenograft (data not shown). Figure 1D shows a double staining of an SKMEL-28 human melanoma xenograft section using L19 (red) and a monoclonal recognizing the murine CD31, a marker of endothelial cells (brown). It is possible to see the endothelial cells surrounded by B-FN.

The SKMEL-28 human melanoma, when injected subcutaneously in nude mice, grows exponentially as a solid tumor for 25 to 35 days, followed by a very slow growing phase for about 15 or more days. These two phases could be monitored both by (1) measuring the size of the tumor at different days after cell injection, and by (2) staining sections with the MoAb KI67, which is specific for cells in proliferation and allows the estimation of the proliferative activity of the tumor. Figure 2A and B shows a double staining, using L19 (red) and the KI67 (brown), of SKMEL-28 xenograft section during the exponentially growing phase (15 days after injection of the cells) and in the quiescent phase (40 days after injection of the cells), respectively. While in the exponentially growing tumor both B-FN-positive vascular structures and a high number of cells in the duplicative phase can be observed, in the section from the quiescent tumor neither B-FN nor proliferating cells are detectable. Furthermore, using L19 (red) and an MoAb specific for the endothelial cells marker CD31 (brown) for immunostaining, vascular structures surrounded by B-FN were clearly visible in exponentially growing phase of the SKMEL-28 tumor (Fig 2C), while the vascular structures did not show any presence of B-FN in the quiescent phase (Fig 2D).

To investigate whether the high-affinity L19 antibody was able to efficiently localize in tumoral vessels *in vivo* after intravenous injection, we performed biodistribution experiments in mice bearing a F9 teratocarcinoma, a rapidly growing murine tumor.¹⁴ Blood vessels of F9 tumors are strongly stained by scFv(L19) *in vitro* using immunohistochemical techniques (Fig 1A), and represent only a small percent of the total tumoral mass.¹¹ Radioiodinated scFv(L19) or scFv(D1.3) (an irrelevant antibody specific for hen egg lysozyme) were injected in the tail vein of mice with subcutaneously implanted F9 tumors, and antibody biodistributions were obtained at different time points (Fig 3; Table 1). ScFv(L19) is rapidly eliminated from blood through the kidneys, with a typical biphasic profile.²³

Eight percent of the injected dose per gram of tissue (%ID/g) already localizes in the tumor 3 hours after injection. The subsequent decrease of antibody dose amount is in part due to the fact that the tumor doubles in size in approximately 48 hours (Fig 4). The kinetic dissociation constant (k_{off}) of the ^{125}I -labeled L19/ED-B complex was too low to be measured by real-time interaction analysis with surface plasmon resonance detection (Fig 5A), and was therefore measured by a competition experiment (Fig 5B). The k_{off} value measured ($6.8 \times 10^{-5} \text{ s}^{-1}$) is somewhat higher than the value measured for the nonradioiodinated L19,¹⁸ and corresponds to a half-life of the antibody-antigen complex of 2.8 hours ($T_{1/2} = 0.69/k_{\text{off}}$)²⁴ in conditions of irreversible dissociation and in the absence of rebinding. However, it has previously been shown that rebinding effects determine a longer residence time of antibody fragments on tumor than the one predicted by the k_{off} value.²⁵

Tumor:blood ratios at 3, 5, and 24 hours after injection were 1.9, 3.7, and 11.8, respectively, for L19, but always below 1.0 for the negative control antibody. Unlike conventional antibodies, scFv(L19) does not accumulate in the liver or other organs, with %ID/g values at 24 hours for the main organs ranging between 0.02 and 1 (Table 1). The localization of L19 at the level of vascular structures was confirmed by microradio-

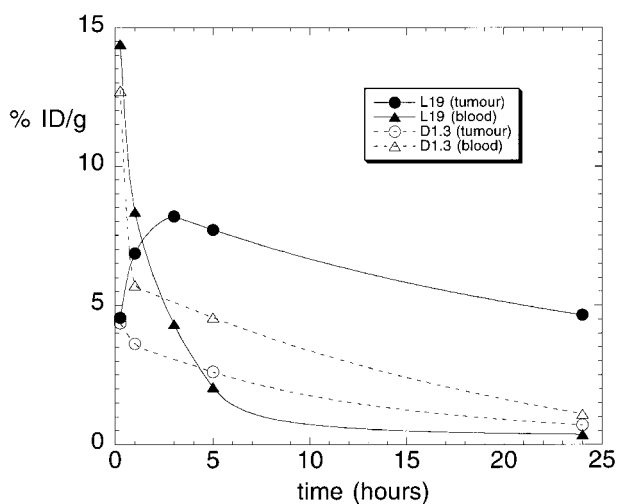


Fig 3. Tumor-targeting performance of recombinant antibody fragments. Results of biodistribution studies in nude mice bearing a subcutaneously implanted F9 murine teratocarcinoma, performed with radiolabeled scFv(L19) and scFv(D1.3). Tumor and blood levels are expressed as percent injected dose per gram (%ID/g).

Table 1. Biodistributions of Radiolabeled L19 and D1.3 Antibody Fragments in Tumor-Bearing Mice

%ID/g										
Time (h)	Kidney	Spleen	Lung	Liver	Blood	Tumor	Femur	Heart	Muscle	
scFv (L19)										
0.25	26.4 ± 4.7	5.4 ± 0.4	15.1 ± 5.1	5.7 ± 0.6	14.4 ± 2.6	4.6 ± 1.1	3.1 ± 0.6	5.7 ± 0.9	1.1 ± 0.3	
1	19.2 ± 3.9	3.8 ± 0.3	9.8 ± 0.9	2.8 ± 0.3	8.3 ± 0.9	6.9 ± 2.4	3.5 ± 0.6	4.0 ± 0.5	0.9 ± 0.3	
3	8.1 ± 1.6	2.0 ± 0.3	5.0 ± 1.4	1.7 ± 0.02	4.3 ± 0.3	8.2 ± 4.2	2.9 ± 0.6	2.1 ± 0.3	1.1 ± 0.1	
5	4.2 ± 1.1	1.8 ± 0.2	3.5 ± 0.2	1.3 ± 0.3	2.1 ± 1.6	7.7 ± 2.5	2.4 ± 0.4	1.5 ± 0.4	0.9 ± 0.1	
24	0.7 ± 0.1	0.4 ± 0.1	1.0 ± 0.3	0.2 ± 0.04	0.4 ± 0.1	4.7 ± 0.6	1.0 ± 0.06	0.21 ± 0.07	0.2 ± 0.07	
scFv (D1.3)										
0.25	46.5 ± 9.4	5.0 ± 0.5	6.3 ± 1.0	7.8 ± 0.6	12.7 ± 0.1	4.4 ± 1.4	2.6 ± 0.1	4.4 ± 0.9	1.4 ± 0.3	
1	16.5 ± 2.2	2.6 ± 0.5	4.1 ± 1.1	3.1 ± 0.6	5.7 ± 0.7	3.6 ± 1.0	1.7 ± 0.4	2.1 ± 1.6	1.0 ± 0.3	
3	ND	ND	ND	ND	ND	ND	ND	ND	ND	
5	4.7 ± 0.6	1.8 ± 0.5	3.0 ± 0.6	2.6 ± 0.6	4.6 ± 1.2	2.6 ± 1.5	1.6 ± 0.5	1.8 ± 0.4	0.8 ± 0.3	
24	1.5 ± 0.5	0.6 ± 0.2	0.8 ± 0.4	1.1 ± 0.3	1.1 ± 0.5	0.7 ± 0.4	0.2 ± 0.3	0.4 ± 0.2	0.2 ± 0.1	

Biodistribution studies were performed as described in Materials and Methods.

Abbreviations: %ID/g, percent of antibody injected dose per gram of tissue; ND, not determined.

graphic analysis. Figure 6 (see page 194) clearly shows accumulation of the radiolabeled antibody in the blood vessels of the F9 mouse tumor, but not in the vessels of the normal tissue surrounding the tumor. No accumulation of radiolabeled antibody was detected in the vessels of other organs (liver, lung, muscle, spleen, kidney, brain, and skin) of the tumor-bearing mice (data not shown).

We further investigated whether the targeting properties of scFv(L19) were dose-dependent, performing a biodistribution analysis at 24 hours after intravenous injection of 0.7 to 10 μg ^{125}I -labeled L19 (1 μCi per μg of antibody fragment). In the dose range tested, the tumor-targeting property of L19, expressed as %ID/g, remained essentially constant (Fig 7). These results are consistent with the fact that the initial antibody concentration in blood, even at the lower dose injected [for 2 mL of blood: Molar Concentration = mg of L19/(Blood Volume \times Molecular Weight) = 0.0007/(2 \times 30,000) = 11.2 nmol/L], was significantly higher than the antibody dissociation constant, which lies in the sub-nanomolar range.^{18,24}

DISCUSSION

The immunohistochemistry experiments reported here, performed using four different tumor animal models, have shown

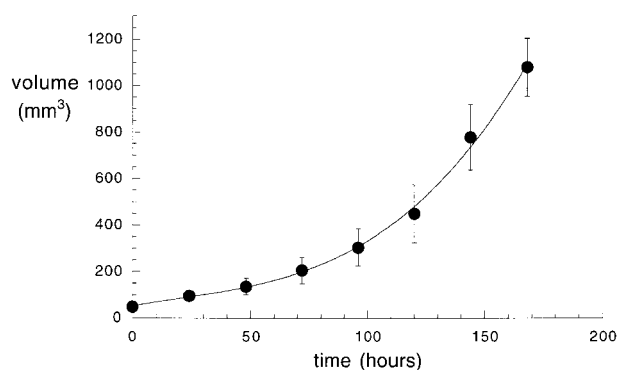


Fig 4. Velocity of the growth of grafted F9 teratocarcinoma in nude mice. The volume of F9 tumors in nude mice is plotted versus time, showing a doubling time of approximately 48 hours. Data points are averages of 10 mice; standard deviations are indicated.

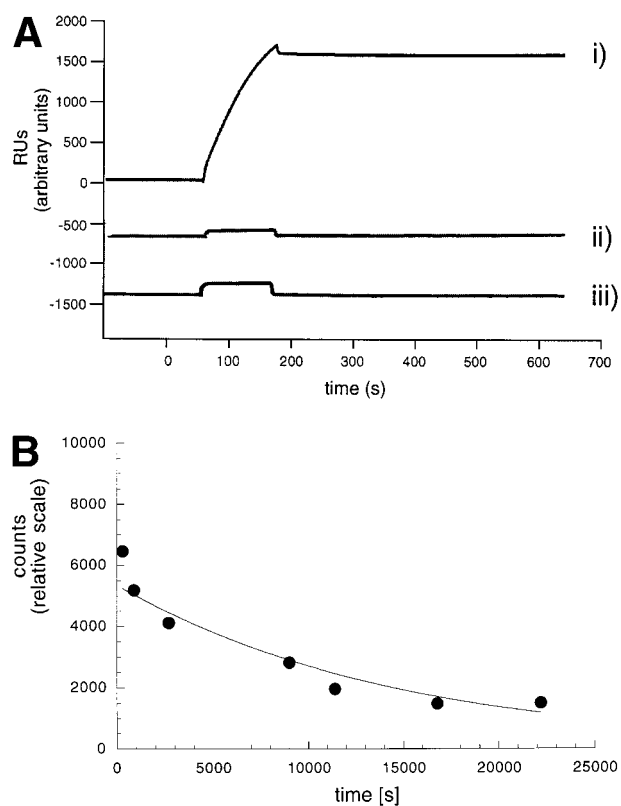


Fig 5. Kinetic stability of the L19 / ED-B complex. (A) Real-time interaction analysis of the antigen binding properties of antibody solutions detected using a BIAcore instrument. (i) ScFv(L19) binding to recombinant ED-B immobilized on a microsensor chip. Note that after the initial baseline, the antibody binding to the antigen is detected as an increase of resonance units (RUs). The following flat dissociation profile demonstrates the kinetic stability of the complex. (ii) scFv(D1.3) binding to the ED-B-coated sensor chip of (i). (iii) scFv(L19) binding to a microsensor chip coated with hen egg lysozyme. Specific antigen binding is detected only in sensorgram (i). (B) Measurement of the kinetic dissociation constant of ^{125}I -labeled L19/ED-B complex immobilized on a microtiter plate, by competition of the complex with a molar excess of unlabeled recombinant ED-B and radioactive counting (see Materials and Methods).

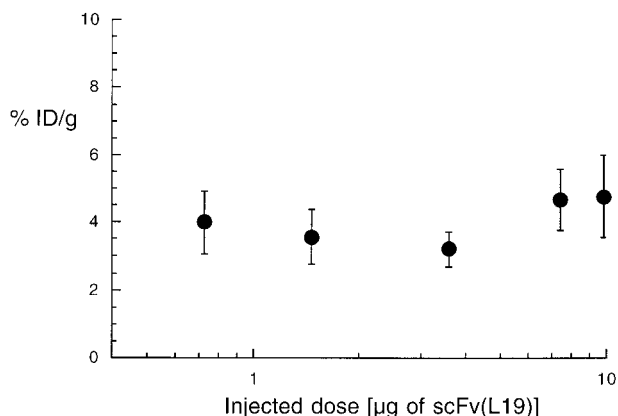


Fig 7. Dose-response dependence of the tumor-targeting properties of scFv(L19). Plot of the percent of injected dose per gram of tumor (%ID/g) obtained with different doses of radiolabeled L19 (activity: 1 μ Ci per μ g of antibody). The tumor targeting performance of the antibody is essentially constant over this concentration range.

that B-FN accumulates around vasculature structures during angiogenic processes, but is undetectable in mature vessels. These results are in keeping with our previous results⁹⁻¹¹ and with a recent study performed by a different group,²⁶ which has shown that B-FN is present around the blood vessels of human skin tumors only during angiogenic processes.

The tumor-targeting results obtained show that new-forming blood vessels can be distinguished from mature vessels *in vivo* after intravenous injection. They also indicate that a radiolabeled high-affinity anti-ED-B antibody, injected at a distant site in tumor-bearing mice, rapidly finds its way to the tumor and preferentially localizes in it. Three hours after injection, the dose of antibody in the tumor was higher than the dose in the other organs (Table 1).

From Fig 3 we can derive that the area under the curve (AUC) of the radioactivity delivered by L19 to the tumor during the first 24 hours is 3.6-fold higher than the AUC for blood. This ratio increases when the AUC is measured for longer time periods. Because new-forming blood vessels in F9 teratocarcinoma constitute less than 5% of the total tumor mass,¹¹ the radioactivity delivered to vascular structures is significantly higher (>70-fold) than the one delivered to normal tissues and blood.

Because the biodistribution studies were performed using radioiodinated antibodies, dehalogenation occurs *in vivo*, as it can be seen by the accumulation of the radionuclide in the stomach and in the thyroid (1.5 and 1.2 %ID/g at 24 hours, respectively; data not shown). Accordingly, estimates of tumor retention may be artificially low.

ScFv(L19) could be useful for the selective delivery of suitable therapeutic radionuclides or other toxic agents to tumoral vasculature. Antibodies to angiogenesis markers are suitable for targeting several different tumor types, because new-forming blood vessels are a general feature of tumoral progression and invasion. Cells of new-forming vessels, unlike tumor cells, do not mutate and, therefore, the antigens associated to angiogenesis are a constant feature. Destruction or occlusion of tumoral vessels may result in tumor collapse and infarction.^{2-8,12} Moreover, the targeting of new-forming blood

vessels with anti-ED-B reagents appears not to be limited to tumoral angiogenesis. Indeed, we have recently shown that new blood vessels experimentally induced in rabbit eyes are rich in ED-B (Birchler M, Viti F, Zardi L, Spiess B, Neri D: submitted), opening opportunities for targeted drug delivery in ocular disorders associated with neovascular proliferation.

The results presented in this report suggest an avenue toward the detection of angiogenesis in patients with cancer by immunoscintigraphic techniques. The development of antibody fragments with very high affinity toward the ED-B domain of fibronectin has yielded agents capable of homing rapidly and in large amounts in tissues undergoing angiogenesis. This feature is an essential prerequisite for scintigraphic applications, in which short-lived radionuclides such as ^{99m}Tc or ¹²³I have to be used to minimize exposure of the patients to radiation.

REFERENCES

1. Folkman J: Angiogenesis in cancer, vascular, rheumatoid and other disease. *Nat Med* 1:27, 1995
2. O'Reilly MS, Holmgren L, Chen C, Folkman J: Angiostatin induces and sustains dormancy of human primary tumors in mice. *Nat Med* 2:689, 1996
3. O'Reilly MS, Boehm T, Shing Y, Fukai N, Vasios G, Lane WS, Flynn E, Birkhead JR, Olsen BR, Folkman J: Endostatin: An endogenous inhibitor of angiogenesis and tumor growth. *Cell* 88:277, 1997
4. Friedlander M, Brooks PC, Shaffer RW, Kincaid CM, Varner JA, Cheresch DA: Definition of two angiogenic pathways by distinct alpha-integrins. *Science* 270:1500, 1995
5. Pasqualini R, Koivunen E, Ruoslahti E: Alpha-v integrins as receptors for tumor targeting by circulating ligands. *Nat Biotechnol* 15:542, 1997
6. Huang H, Molema G, King S, Watkims L, Edgington TS, Thorpe P: Tumour infarction in mice by antibody-directed targeting of tissue factor to tumor neo-vasculature. *Science* 275:547, 1997
7. Kim KJ, Li B, Winer J, Armanini M, Gillett N, Phillips HS, Ferrara N: Inhibition of vascular endothelial growth factor-induced angiogenesis suppresses tumour growth *in vivo*. *Nature* 362:841, 1993
8. Schmidt-Erfurth U, Diddens H, Birngruber R, Hasan T: Photodynamic targeting of human retinoblastoma cells using covalent low-density lipoprotein conjugates. *Br J Cancer* 75:54, 1997
9. Castellani P, Viale G, Dorcaratto A, Nicolò G, Kazmarek J, Querze G, Zardi L: The fibronectin isoform containing the ED-B oncofetal domain: A marker of angiogenesis. *Int J Cancer* 59:612, 1994
10. Kazmarek J, Castellani P, Nicolò G, Spina B, Alemanni G, Zardi L: Distribution of oncofetal fibronectin isoforms in normal, hyperplastic and neoplastic human breast tissues. *Int J Cancer* 58:11, 1994
11. Carnemolla B, Neri D, Castellani P, Leprini A, Neri G, Pini A, Winter G, Zardi L: High-affinity human recombinant antibodies to the oncofetal angiogenesis marker fibronectin ED-B domain. *Int J Cancer* 68:397, 1996
12. Neri D, Zardi L: Affinity reagents against tumour-associated extracellular molecules and new-forming blood vessels. *Adv Drug Deliv Rev* 31:43, 1998
13. Huston JS, Levinson D, Mudgett HM, Tai MS, Novotny J, Margolies MN, Ridge RJ, Brucoleri RE, Haber E, Crea R, Oppermann H: Protein engineering of antibody binding sites: recovery of specific activity in an anti-digoxin single-chain Fv analogue produced in *Escherichia coli*. *Proc Natl Acad Sci USA* 85:5879, 1988
14. Neri D, Carnemolla B, Nissim A, Balza E, Leprini A, Querze G, Pini A, Tarli L, Halin C, Neri P, Zardi L, Winter G: Targeting by affinity-matured recombinant antibody fragments of an angiogenesis associated fibronectin isoform. *Nat Biotechnol* 15:1271, 1997

15. Corbett TH, Griswold DPJ, Roberts BJ, Peckham JC, Schabel FMJ: Tumor induction relationships in development of transplantable cancers of the colon in mice for chemotherapy assays, with a note on carcinogen structure. *Cancer Res* 35:2434, 1975
16. Carney DN, Gazdar AF, Bepler G, Guccion JG, Marangos PJ, Moody TW, Zweig MH, Minna JD: Establishment and identification of small cell lung cancer cell lines having classic and variant features. *Cancer Res* 45:2913, 1985
17. Vecchi A, Garlanda C, Lampugnani MG, Resnati M, Matteucci C, Stoppacciaro A, Schnurch H, Risau W, Ruco L, Mantovani A, Dejana E: Monoclonal antibodies specific for endothelial cells of mouse blood vessels. Their application in the identification of adult and embryonic endothelium. *Eur J Cell Biol* 63:247, 1994
18. Pini A, Viti F, Santucci A, Carnemolla B, Zardi L, Neri P, Neri D: Design and use of a phage-display library: human antibodies with subnanomolar affinity against a marker of angiogenesis eluted from a two-dimensional gel. *J Biol Chem* 273:21769, 1998
19. Harper M, Lema F, Boulot G, Poljak RJ: Antigen specificity and cross-reactivity of monoclonal anti-lysozyme antibodies. *Mol Immunol* 24:97, 1987
20. Salacinski PRP, McLean C, Sykes JEC, Clement-Jones VV, Lowry PJ: Iodination of proteins, glycoproteins, and peptides using a solid-phase oxidizing agent, 1,3,4,6-tetrachloro-3 α ,6 α -diphenyl glycoluril (Iodogen). *Anal Biochem* 117:136, 1981
21. Mariani G, Lasku A, Balza E, Gaggero B, Motta C, Di Luca L, Dorcaratto A, Viale G, Neri D, Zardi L: Tumor targeting potential of the monoclonal antibody BC-1 against oncofetal fibronectin in nude mice bearing tumor implants. *Cancer* 80:2378, 1997
22. Winter G, Griffiths AD, Hawkins RE, Hoogenboom HR: Making antibodies by phage display technology. *Annu Rev Immunol* 12:433, 1994
23. Begent RHJ, Verhaar MJ, Chester KA, Casey JL, Green AJ, Napier MP, Hope-Stone LD, Cushen N, Kepp PA, Johnson CJ, Hawkins RE, Hilson AJW, Robson L: Clinical evidence of efficient tumor targeting based on single-chain Fv antibody selected from a combinatorial library. *Nat Med* 2:979, 1996
24. Neri D, Montigiani S, Kirkham PM: Biophysical methods for the determination of antibody-antigen affinities. *Trends Biotechnol* 14:465, 1996
25. Adams GP, Schier R, Marshall K, Wolf EJ, McCall AM, Marks JD, Weiner LM: Increased affinity leads to improved selective tumor delivery of single-chain Fv antibodies. *Cancer Res* 58:485, 1998
26. Karelina TV, Eisen AZ: Interstitial collagenase and the ED-B oncofetal domain of fibronectin are markers of angiogenesis in human skin tumors. *Cancer Detect Prev* 22:438, 1998